JOURNAL OF AGRICULTURAL AND FOOD CHEMISTRY

Article

pubs.acs.org/JAFC

Synthesis of Resins with Ionic Liquids for Purification of Flavonoids from *Hippophae rhamnoides* L. Leaves

Song Lou[†,‡] and Duolong Di*[,†,#]

[†]Key Laboratory of Chemistry of Northwestern Plant Resources and Key Laboratory for Natural Medicine of Gansu Province, Lanzhou Institute of Chemical Physics, Chinese Academy of Sciences, Lanzhou 730000, People's Republic of China

[‡]Graduate University of the Chinese Academy of Sciences, Beijing 100049, People's Republic of China

[#]Centre of Resource Chemical and New Material, Lanzhou Institute of Chemical Physics, Chinese Academy of Sciences, Qingdao 266100, People's Republic of China

ABSTRACT: The efficient purification method of high-purity flavonoids from *Hippophae rhamnoides* L. (sea buckthorn) is reported. A novel room temperature ionic liquid-based macroporous adsorption resin (MAR), *N*-methylimidazole/MARs (Mim/MARs), was prepared on the basis of the Friedel−Crafts-catalyzed and surface-modified technique. The material exhibited favorable characteristics for adsorption application, including high pore volume (1.90 cm^3/g, 3 times as big as the optimal commercial adsorbent), good pore structure (type IV isotherm with an H1 hysteresis loop, the most favorable structure for adsorption purposes), narrow particle size and pore size distribution (1.2 mm with a standard deviation of 0.106 mm), and excellent chemical stability. This paper also presents the first experimental evidence that the functional groups of the modified materials and composite action of certain molecular interactions between the adsorbent and flavonoids affected the adsorption process. Moreover, a new sphere-size adsorption kinetics model in which the adsorption process contained three or more compartments and detailed parameters of sphere size was developed according to the multicompartment kinetics model and Karichhoff's theory by investigating the regression of the experimental results. The conclusion that the first compartment of the adsorption process onto Mim/MARs mainly occurred on spheres larger than 0.83 mm and the second and third ones mainly occurred on spheres of 0.46−0.83 and 0.22−0.46 mm, respectively, was drawn from this new sphere-size adsorption kinetics model.

KEYWORDS: *ionic liquids, macroporous adsorption resins, separation, flavonoids, Hippophae rhamnoides L. leaves*

INTRODUCTION

Hippophae rhamnoides L. (sea buckthorn), a thorny, nitrogen-fixing, deciduous shrub with very high nutraceutical and therapeutical values, is naturally distributed throughout Asia, Europe, and North America.[1] Its leaves have a long history of applications in Tibetan, Mongolian, Chinese, and Middle Asian medicines, and it is considered to be a good source of a large number of bioactive substances.[1,2] Recently, the nutritional value of *H. rhamnoides* L. has drawn more attention in North America and Europe.[3,4] Modern medical and chemical studies have shown that flavonoids are the main active components in *H. rhamnoides* L.[5,6] According to modern pharmacology research, flavonoids from *H. rhamnoides* L. have anti-inflammatory, antitumor, antioxidant, and free-radical scavenging properties, and they also have been widely used in the research and development of natural medicine as well as in clinical application.[7−9]

Due to the importance of flavonoids in *H. rhamnoides* L. for humans, it was of greater significance to develop a simple separation technique. Adsorption technology is currently being used extensively for the separation of target component and has proven to be one of the most effective techniques for separation and purification from natural plants.[10] Compared with traditional methods of separation such as hot leaching, solvent extraction, and ultrasound-assisted extraction, the macroporous adsorption resins (MARs) are viewed as a more attractive alternative due to their high efficiency, low pollution, and procedural simplicity characteristics.

There have been some reports on the application of the commercial MARs in the enrichment process of flavonoids.[11−18] The matrix of these MARs was usually of polyacrylic or styrene−divinyl benzene ester; the absorption mechanism primarily relied on a hydrophobic force such as the van de Waals force in the aqueous solution, however, which may lead to the low adsorption selectivity.[19] Certain adsorbates, such as flavonoids, have special structures that have multiphenolic groups and a hydrophobic skeleton, as shown in Figure 1. The structure indicates that if some special functional groups are introduced onto the current MAR matrix to activate the hydrogen bond interaction between adsorbents and flavonoids and improve the structure of the pores, higher purity flavonoids may be achieved from the complicated system of natural plants.[20,21]

Recently, room temperature ionic liquids (RTILs) have begun to be used as functional groups of adsorption media in separation. Used in this way, RTILs no longer constituted a new or original solvent. They should be considered as salts most often dissociated in an anion and a cation. Poole and co-workers[22] studied the use of ethylammonium nitrate and propylammonium nitrate in liquid chromatography. Fuller and co-workers[23] fully characterized the low-melting salt 1-ethyl-3-

Received: February 14, 2012
Revised: May 30, 2012
Accepted: June 1, 2012
Published: June 1, 2012

dx.doi.org/10.1021/jf300633g | *J. Agric. Food Chem.* 2012, 60, 6546−6558

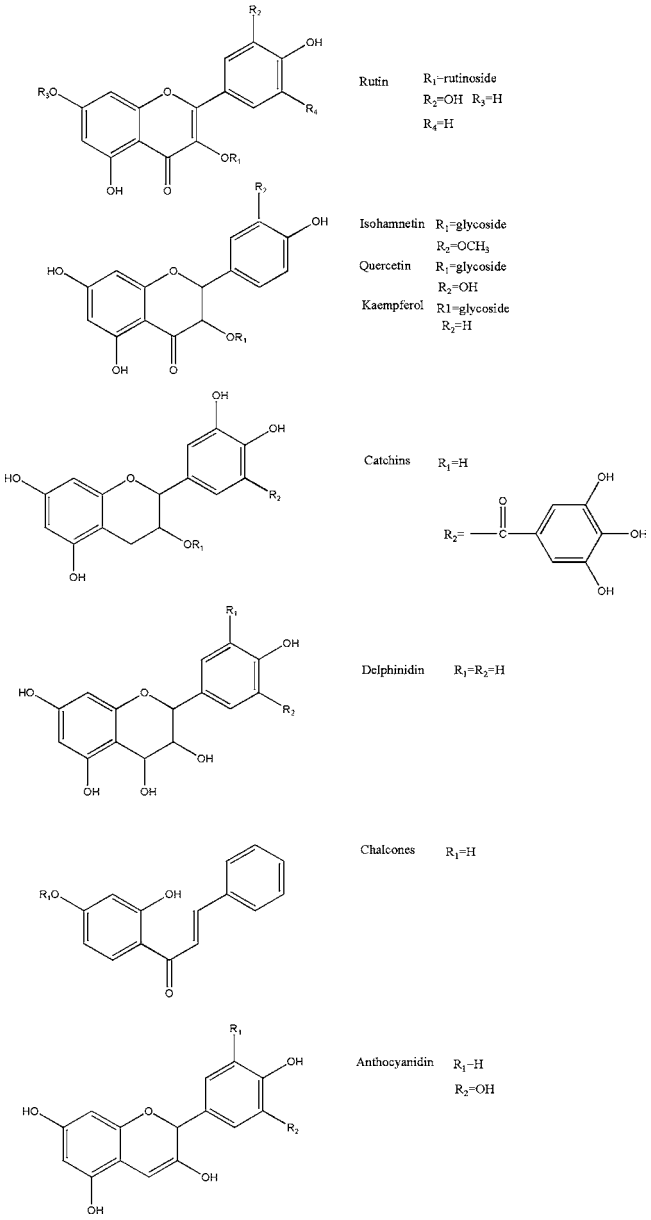

Figure 1. Structures of flavonoids in sea buckthorn.

methylimidazolium hexafluorophosphate (1×10^{-3}, MI-HFP, mp 58−60 °C). They reported that its interionic interactions were dominated by cation−anion Coulombic attraction with minimal hydrogen bonding. Like 1-ethyl-3-methylimidazolium tetrafluoroborate (1×10^{-3}, MI-TFB, mp 15 °C),[24] it is air- and water-stable. In another study, Yanes used 1-alkyl-3-methylimidazolium-based ionic liquids as the sole electrolyte to enable the capillary electrophoretic separation of the phenolic constituents of grape seed extract.[25] Jiang reported the use of ionic liquids as additives in eluents to separate ephedrines, amines, and nucleotides in HPLC. They also studied the preparation of a new anion-exchange phase based on *N*-methylimidazolium-immobilized on silica, which was used as stationary phase in HPLC.[26,27] However, there is no report of the use of RTILs as adsorbate selector in resin.

The introduction of of RTILs onto current MAR matrix could activate not only the hydrogen bond interaction but also multiple interactions, including hydrophobic interactions, ion−dipole, and ion-induced−dipole, between adsorbent and adsorbate to improve the separation and purification.

The focus of this paper was the fabrication of an ionic liquid on micrometer-scale MARs and its adsorption capacity for flavonoids from *H. rhamnoides* L. leaves. To probe the effect of sphere size on the adsorption process, we supposed a new adsorption kinetics model. The pattern in which the adsorption process contained more compartments and more detailed parameters of sphere size was proposed according to Fickian's theory.[28−30] The results showed that the adsorption selectivity of the synthesized MARs was better, and the sphere size apparently affected the adsorption process.

EXPERIMENTAL PROCEDURES

Chemicals and Materials. MAR spheres were synthesized according to the suspension polymerization method. The average particle size was 0.15 mm with a deviation of 0.0138 mm. The specific surface area, pore volume, and pore diameter were 459 m^2/g, 1.40 cm^3/g, and 12.1 nm, respectively. Pharmaceutical grade chloromethyl methyl ether was purchased from Jinan Leqi Chemical Reagent Co., Inc. (Shandong province, China), and chemical grade *N*-methylimidazole from Shanghai No. 4 Chemical Reagent Co., Inc. (Shanghai, China); analytical grade methanol, sodium chloride, dichloromethane, triothylenetetramine, zinc chloride, sodium chloride, acetonitrile and all solvents used in this paper were purchased from Tianjin Chemical Reagent Co., Inc. (Tianjin, China), and distilled water was prepared in our laboratory. The *H. rhamnoides* L. leaves were obtained from Gansu Greenness Biotech Co., Ltd. (Gansu province, China), and they were employed after washing and drying. The standards were purchased from the National Institutes for Food and Drug Control (Beijing, China).

Ionic Liquid on Micrometer-Scale MARs (RTILs/MARs). The titled adsorbent was first prepared on the basis of the Friedel−Crafts catalysis and then followed by derivatization via pendant chlorine groups onto mirometer-scaled MARs. Scheme 1 outlines the procedure.

The preparative process has three major steps. First, the surface of MAR particles are treated prior to use. The weighed initial MAR sphere (MARs of polystyrenes with no functional groups) were pretreated by soaking in ethanol overnight and subsequently washed thoroughly by distilled water to remove the monomers and porogenic agents trapped inside the pores during the synthesis process. Second, the MAR sphere is grafted with chloromethylation reagent (Cl/MARs). The dried MAR particles were soaked in dichloromethane for 24 h and then added into a solution containing dichloromethane, zinc chloride initiator, and sodium chloride in a 1000 mL three-necked round-bottom flask equipped with a mechanical stirrer, a reflux condenser, and a thermometer. The round-bottom flask was heated with a programmed heater. The mixture was stirred to give a suspension of beads of a suitable size in the solution (100−120 rpm) and then held at 323 K for 20 h for the grafting of chloromethyl onto the core particles to form a surfactant film, followed by a careful washing procedure to remove the physically adsorbed regent with distilled water and methanol until there was no white precipitate while an aqueous solution of silver nitrate was added into the filtrate. Third, *N*-methylimidazole (RTILs) was grafted on MARs. Cl/MARs were dried, swelled with acetonitrile for 24 h, and added into a solution containing *N*-methylimidazole and acetonitrile in a 1000 mL three-necked round-bottom flask equipped with a mechanical stirrer, a reflux condenser, and a thermometer. The mixture was held at 353 K for 48 h under the protection of nitrogen for the grafting of *N*-methylimidazole onto the core particles to form a novel MAR modified by RTILs, and it was washed with ethyl acetate until there was no white precipitate while an aqueous solution of silver nitrate was added to the filtrate.

Determination of the Number of Chloromethyl Groups and *N*-Methylimidazole in Adsorbents. The number of chloromethyl groups and *N*-methylimidazole groups before and after reactions were determined according to an electrochemistry method. The synthetic beads were weighed, heat-digested, and diluted in distilled water for a testing of electric potential. The electrochemistry workstation was

dx.doi.org/10.1021/jf300633g | J. Agric. Food Chem. 2012, 60, 6546−6558

Scheme 1. Preparation Steps for Mim/MAR Adsorbents

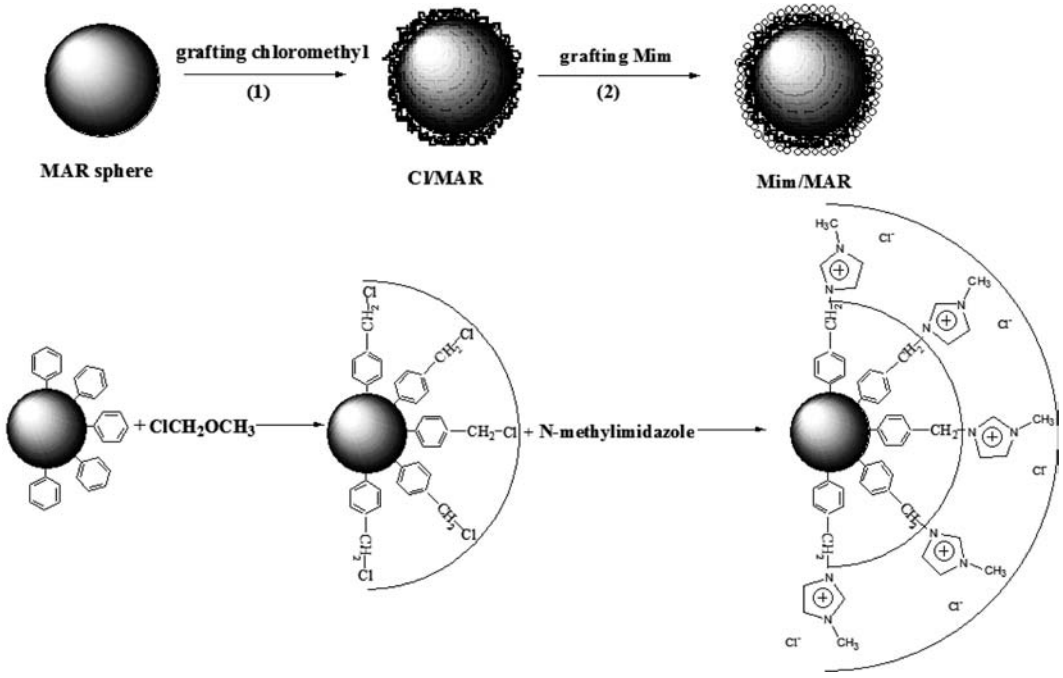

composed of a potentiometer (PHS-3D, Shanghai Precision and Scientific Instrument Co., Ltd., Shanghai, China) and chloride and calomel selectivity electrodes. The standard curve of the amount of chloromethyl was drawn according to a standard solution of sodium chloride at different concentrations.[31]

Instrumentation. X-ray photoelectron spectroscopy (XPS) was used to evaluate the functional groups of modified resins. The spectra were recorded on an Escalab 210 Axis Ultra photoecectron spectrometer (VG Scientific, East Grinstead, U.K.) using Mg Kα as excitation source. The specific surface area, pore volume, and pore size distribution of the adsorbents were calculated according to the BET and BJH methods, respectively, via the nitrogen adsorption and desorption curves at 77 K using a Micromeritics ASAP2020 automatic surface area and porosity analyzer (Micromeritics Instrument Corp., Atlanta, GA, USA). Before the BET surface area measurement, the adsorbents were outgassed at 333 K for 24 h on the degas port of the analyzer. Infrared spectra of the adsorption resins were obtained from a Nexus-670 FT-IR spectrometer (Nicolet, Madison, WI, USA) with a pellet of powdered potassium bromide and adsorbent in the range of 500−4000 cm^{-1}. Carbon, hydrogen, and nitrogen contents (in percentages) of Cl/MARs and Mim/MARs were determined on a Vario EL (Elementar, Hanau, Germany).

Preparation of Sample Solutions. *H. rhamnoides* L. leaves (1 kg) were extracted with 12 L of distilled water in a bath at 353 K for 2 h; this extraction was repeated with 8 L of distilled water. The double extracts were mixed and negative pressure filtered, the filtrate was evaporated to yield the fluid extract of 6 L of ethanol (95%, v/v) added followed by standing for 24 h, and the supernatant of the solution was evaporated to yield the fluid extract by removing the ethanol under reduced pressure in a rotary evaporator (RE-52C, Gongyi City Yuhua Instrument Co., Ltd., China) at 323 K. The extract of *H. rhamnoides* L. leaves was photophobically stored in a refrigerator at 253 K. Then the extract was thawed at ambient temperature before use and diluted to an appropriate concentration with distilled water to produce sample solutions.

Adsorption/Desorption Experiments. An adsorption system was constructed with sample solution, pump, adsorption resins, and SHA-B incubator (Scheme 1). In the adsorption process, 100 mL of sample solution with a known concentration (initial concentration) was pumped into a 250 mL conical flask (MAR column) with 1.2 g of dry MARs. Subsequently, the flask was continually shaken in a SHA-B incubator (100 rpm, Jintan Zhengji Instrument Co., Ltd., Jiangsu province, China) at 308 K for 6 h. The concentration of flavonoids (equilibrium concentration) in the drain was analyzed with a UV spectrophotometer. The experiments of desorption were carried out as follows: 50 mL of ethanol (70%, v/v) was pumped into a flask with adsorbate-laden MARs after the adsorption had reached equilibrium. The flask was shaken (100 rpm) at a constant temperature of 303 K for 6 h. Then a corresponding concentration of flavonoids (concentration of desorbed solution) was analyzed with a UV spectrophotometer. The ratios and adsorption/desorption capacities were calculated with the following equations.

adsorption ratio:

$$A\ (\%) = \frac{C_0 - C_e}{C_0} \times 100\% \tag{1}$$

adsorption capacity:

$$q_e = (C_0 - C_e) \times \frac{V_i}{(1 - \alpha)W} \tag{2}$$

A is the adsorption ratio (%) and q_e is the adsorption capacity (mg/g of dry resin) at adsorption equilibrium. C_0 and C_e are the initial and equilibrium concentrations of the sample solutions, respectively (mg/L). α is the moisture content of the resin (%). W is the weight of the resin used (g). V_i is the volume of sample solution used in the study (mL).

desorption ratio:

$$D\ (\%) = C_d \times \frac{V_d}{(C_0 - C_e)V_i} \times 100\% \tag{3}$$

D is the desorption ratio (%), and q_d is the desorption capacity (mg/g of dry resin) after desorption equilibrium. C_d is the sample concentration in the desorption solution (mg/L). V_d is the volume of the desorption solution (mL). C_0, C_e, α, W, and V_i are the same as defined above.

The detailed procedures of experiment/desorption experiments and determination of accuracy and precision were reported previously.[32,33] The values of the coefficient of recovery (P) and the relative standard

deviation (RSD) in the experiment were 91.17 and 0.53%, respectively, which indicated that the accuracy and precision could satisfy the needs of the experiment.

Determination of the Flavonoids. Flavonoids in the aqueous solution were determined by using a UV spectrophotometer (T-6, Beijing Purkinje General Instrument Co., Ltd., Beijing, China) at a wavelength of 500 nm. The method was in accordance with the Chinese pharmacopoeia. The concentration of flavonoids was determined by the obtained standard plotted in the range of 0.007−0.04 mg/mL: $A = 11.42C - 0.0065$ ($R^2 = 0.9998$), where A and C are the absorbance and the concentrations of flavonoids (mg/mL), respectively.

Adsorption Kinetics Model. The well-known Lagergren pseudo-first-order and pseudo-second-order models were employed to fit the data.

pseudo-first-order kinetics model:

$$\lg(q_e - q_t) = -\frac{K_1}{2.303}t + \lg q_e \quad (4)$$

pseudo-second-order kinetics model:

$$\frac{t}{q_t} = \frac{1}{q_e}t + \frac{1}{K_2 q_e^2} \quad (5)$$

q is the adsorption capacity at equilibrium (e) and at any time t (mg/g dry resin), respectively. The parameters K_1 (min^{-1}) and K_2 (g/(mg min)) are the rate constants of the pseudo-first-order and pseudo-second-order for the adsorption process, respectively.

A phenomenological first-order, two-component, four-parameter model comprising both fast and slow adsorption steps was often used to describe the adsorption rate of adsorbate from adsorbents:[34]

$$\frac{q_{dt}}{q_{de}} = F_1 \exp(-k_s t) + (1 - F_1)\exp(-k_r t) \quad (6)$$

q_{dt} is the solid-phase sorbate concentration at a given time, q_{de} is the initial solid-phase sorbate concentration, and F_1 and $(1 - F_1)$ are the slowly and rapidly adsorbing fractions, respectively. The rate constants of rapid and slow adsorption are designated k_s and k_r (min^{-1}). This model is widely applied in various adsorption systems because of its simplicity and was found to be adequate in describing the adsorption of various samples with different characteristics. The parameters from the model are useful for distinguishing between rapidly and slowly adsorbing fractions. Furthermore, results from the models gave the biphasic nature of adsorption data in study. However, it should be noted that this model does not necessarily consider the reasonable procedures of adsorption. The model defining the adsorption process contained just two steps without taking into account the differences between fast adsorption, slow adsorption, and even slower adsorption. Moreover, all of the models above of adsorption kinetics overlook the extensional delivery parameter and use a constant instead.

In this work, considering the restriction above, a new adsorption kinetics model was created according to Karickhoff's theory, Fickian's theory, and our previous works.[32] The pattern in which the adsorption process should contain more compartments with parameters of sphere size was proposed. The real sections and relationship between adsorption compartments and sphere size were investigated through regression of the experimental result.

The investigation of the termination of the adsorption and parameters was carried out by using Origin 8.1 software. The process was conducted as follows: (1) Equations that the adsorption effect probably terminated at different compartments with detailed parameters of sphere size were deduced. (2) The real terminated layer of the inductive effect was investigated through regression of the experimental results by multilayer inductive effect model. (3) The results obtained were regressed with the new deduced equations and real terminated layer; the regression result contained the related coefficient (R^2), the diameter of the sphere ($r_1, r_2, ..., r_n$), the diffusion coefficient ($D_{r1}, D_{r1}, ..., D_{rn}$), and the χ^2 distribution. D_{r1}, D_{r2}, ... and $D_{r\ n}$ are the adsorbate diffusion coefficient in the polymer in different adsorption compartments. According to Fick's laws, D is constant in different compartments over the concentration range covered by the experiment. Moreover, the evaluation of D requires independent determination of the particle diameter.

RESULTS

It is well-known that particle diameter, uniformity, specific surface area, pore structure, total pore volume, and pore size of resin are very important parameters of MARs. For Mim/MARs, adsorption properties depend fundamentally on the adsorbent structure. A systematic characterization of Mim/MAR particles was carried out to understand its applications as adsorption materials.

Characterization of Mim/MAR Particles. Infrared spectroscopy is one of the useful tools to identify the chemical modifications proposed in the reaction scheme. The grafting functional groups will have a significant effect on the diffuse reflectance infrared Fourier transformation spectra of the modified adsorbent. Figure 2 displays the FTIR spectra of

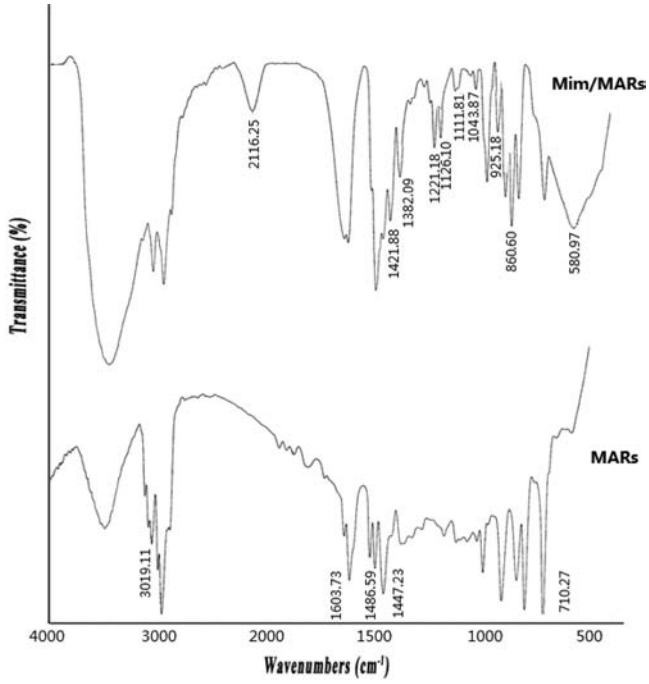

Figure 2. IR spectra of adsorbent original MARs and Mim/MARs.

MARs and Mim/MARs. In the spectrum of MARs, there are some characteristic absorptions of polystyrene, such as the bands at 3019, 1603, 1486, 1447, and 710 cm^{-1}. In the spectrum of Mim/MARs, the N−H structure was disclosed by the occurrence of a band at 860 cm^{-1} as a result of out-of-plane bending vibrations of N−H and a band at 925 cm^{-1} as a result of the rocking vibration of the N−H. There were also some other new absorption bands at 1126, 1221, and 1382 cm^{-1}. They were the stretching vibration of C−N.[35,36] Meanwhile, the spectrum showed MAR resins also had some chloromethyl groups due to the absorption bands at 1036, 1113, and 1246 cm^{-1}.[37] There were also absorption bands in the vicinity of 580 and 2116 cm^{-1}. The first band belonged to the stretching vibrations of the C−Cl bond, and the second one was the in-plane bending vibrations adsorption of the ═C—H bond of the benzene ring after binary

dx.doi.org/10.1021/jf300633g | J. Agric. Food Chem. 2012, 60, 6546−6558

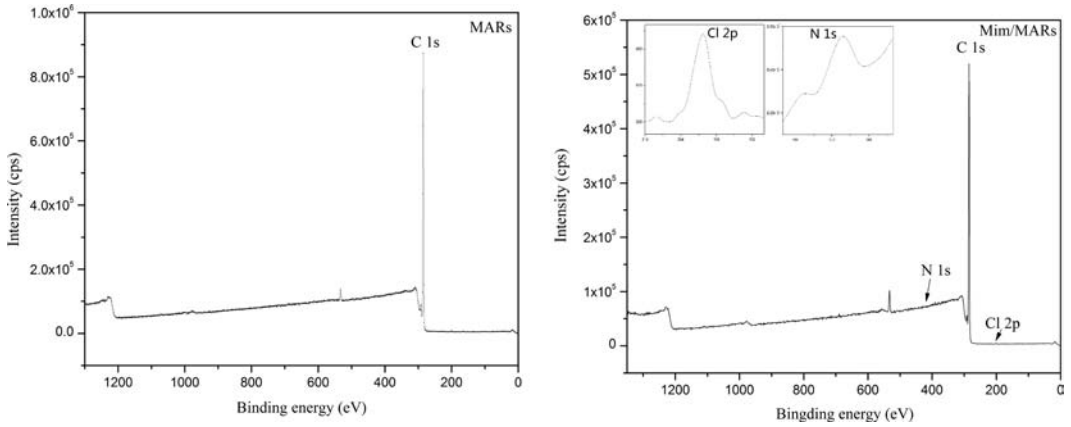

Figure 3. XPS characterization of MARs and Mim/MARs.

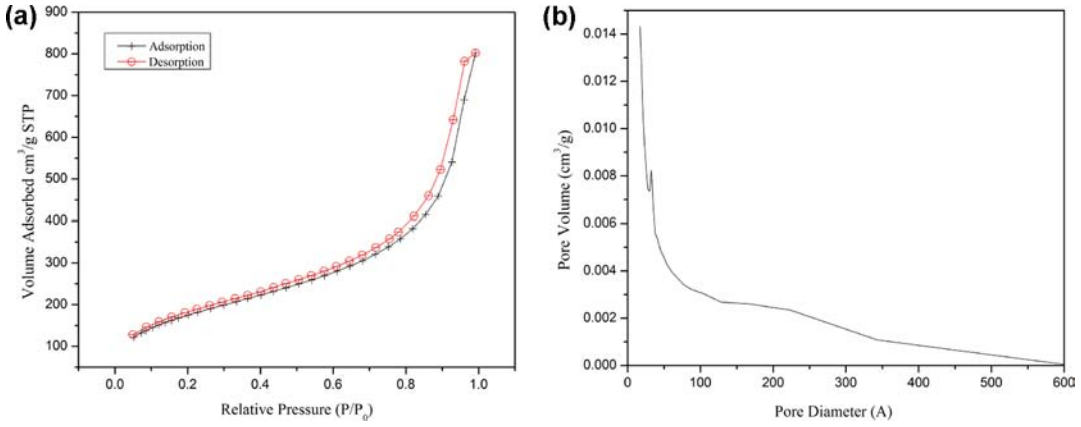

Figure 4. (a) Isotherm and (b) distribution of pore diameter of Mim/MARs.

substitution caused by the substitution of hydrogen atoms at the para position of benzene rings by $-CH_2Cl$.[37]

The characteristic XPS substrate signal (Figure 3) for unmodified MARs (left) at 285 eV was attributed to C 1s. Chlorine (~200 eV), carbon (~285 eV), and nitrogen (~399.5 eV) photoelectron peaks (in order from low to high binding energy) were observed for resins functionalized with *N*-methylimidazole (right). Therefore, the signal evidently showed that *N*-methylimidazole had been grafted onto the MARs. Moreover, the results of XPS signals also showed that modified resins had some rudimentary chloromethyl groups, and the replacement ratio of *N*-methylimidazole groups from chloromethyl groups was 53.67%.

The elemental analysis data also proved that modification on the MARs was successful. In MARs: C, 72.27%; H, 6.44%. In Cl/MARs: C, 65.78%; H 6.09%. In Mim/MARs: C, 43.68%; H, 7.15%; N, 1.05%. From the percentage amounts of carbon and nitrogen, the bonding densities were 0.703 mmol/g for Cl/MARs and 0.376 mmol/g for Mim/MARs, respectively, which agreed with the result of XPS. The results also showed that a little anchored precursor remains on the surface and had not been substituted by *N*-methylimidazole groups.

Surface Parameters of Mim/MAR Particles. The isotherm for Mim/MARs is shown in Figure 4a, which is of a type IV adsorption isotherm with an H1 hysteresis loop according to IUPAC recommendations.[38] The pore size distribution of Mim/MARs is displayed in Figure 4b. The structure parameters of commercial and synthetic resins calculated using the standard BET method are listed in Table 1.

DISCUSSION

Since the possibility of MARs as adsorbent was reported, it has been studied in detail for its separation applications for various types of specific organic compounds. Several methods have been developed for the preparation of MARs used in adsorption.[39] The cross-linking reaction, the mixed-mode method, and the experimental conditions controlled are the most used ones. Nevertheless, there are some limitations in application of MARs prepared according to the methods mentioned above. The disadvantages are chiefly their low specific surface area and pore volume, broad pore size distribution and particle size distribution, and unfavorable pore structure. Meanwhile, theoretical research about the adsorption feature of MARs lags severely at present. To overcome the above impediments, a significant improvement or a novel procedure is needed. The emphasis of this paper is placed on producing an adsorbent with some favorable adsorption properties and creating a reasonable pattern to describe the adsorption property.

Surface Area and Pore Volume. As described above, adsorbents should have relatively high specific surface area and pore volume in order to be coated or bonded with a sufficient amount of sample solution. Whereas many studies have mainly focused on establishing optimal experimental conditions of adsorption, less attention has been paid to such important properties of the adsorbent.

The specific surface area of an adsorbent is generally accepted as one of its most important adsorption parameters. It is worthwhile to compare the commercial and synthetic MARs on

Table 1. Surface Parameters of Commercial and Synthetic Resins

	a_s (m^2/g)	r_p (nm)	v_p (cm^3/g)
AB-8	480	6.44	0.73
ADS-7	100	12	0.62
ADS-8	450	12	0.78
ADS-17	95	10	0.74
D16	200	16	0.66
D2026	40		
D3520	480	8	2.02
D4006	400	6.5	
D4020	540	10	2.8
D4026	420	7	
D8016	400	9	
DA101	480	11	
DA201	250	15	
DA301	30		
DF01	400	7	
DR02	480	13	
H103	700	8.5	0.58
HPD100	400	10	0.44
HPD450	700	13	0.36
HPD722	550	12	0.34
HPD750	700	9	0.36
LSA7	400	20	0.34
LSA10	550	24	0.46
LSA21	600	7.25	0.44
LSA30	560	18	0.43
LSA40	400	26	0.44
LX28	508	24	0.44
LX38	550	26	0.46
LX1180	550	15	0.50
NKA	570	13	0.66
NKA2	160	14	0.87
NKA9	250	10	0.73
NKA12	570	9	
S8	100	28	0.73
X5	500	12	1.08
MAR	500	5.18	0.44
Cl/MAR	513	9.39	1.40
Mim/MAR	649	12.25	1.91

change in their surface area. For most MAR resins (Table 1), surface areas are <500 m^2/g; however, some are >700 m^2/g with much smaller pore size and volume, which are <10 nm and <0.36 cm^3/g, respectively. Unfortunately, the surface area, pore size, and volume of Mim/MARs are >600 m^2/g, >12 nm, and >1.90 cm^3/g, which are about 3 times as big as the optimal commercial adsorbent in physical structure. Carr et al.[40] investigated the changes in surface area and pore volume during thermal treatment of adsorbent and found that the specific surface area depended strongly on the sample's thermal history. The surface area of resins would decrease as the reaction temperature increased. In fact, a temperature higher than 373 K is necessary for the above-mentioned methods in order to increase the grafting ratio of the modified MARs. On the other hand, there are a large number of microporous pores in MARs; this is unfavorable for rapid mass transfer in adsorption, and the separation performance of the resins will deteriorate. In sum, MARs so far always have a low surface area; this will reduce the loading amount of the adsorbate and lead to decreases in adsorbability and selectivity.

The Mim/MAR composite synthesized by the derivatization, however, is a support with high specific surface area and pore volume as shown in Table 1. The high surface area mainly comes from its shell material. In the derivatization, MARs were chosen to be the substrate, which has a lot of micropores. Particle multilayer of nanometer-scale RTILs cation was formed during the modified treatment. Uniform, regular, and ordered arrays of nanostructure pores offer the resin high surface area. Another cause may be its high level of swelling. MARs can be swelled in all kinds of organic solvent. We tested 12 classical kinds of organic solvent, and the result showed that acetonitrile was the best one to swell MARs because of the optimal swelling time and ratio. In our experiments, 353 K was chosen as the reaction temperature not only to keep the lowest loss of organic solvent but to completely increase the grafting ratio and specific area of MARs as well.

The pore volume of MARs particles depends on the size of pores, and the size of the pores is significantly correlated with its sample thermal process. Reaction at temperature higher than 373 K gradually decreases the pore volume of MARs particles from 1.17 to 0.83 g/cm^3. The pore volume of over-cross-linking MARs is generally much lower than that of common resins. The pore volume of Mim/MARs, however, has a value comparable to that of common resins. Reaction temperature, we think, is a key factor to control appropriate pore size and pore volume of MAR-based adsorbent.

As can be seen in Table 1, it is clear that the technique of derivatization which makes the *N*-methylimidazole graft on the matrix of MARs is helpful in preparing a resin with high surface area and pore volume.

Previously, researchers developed modified MAR adsorbent to increase the specific area and pore volume. Wang and co-workers[41] prepared modified MARs (a_s, 94 m^2/g; d_p, 200 μm; r_p, 1.5 nm) by introducing some prevalent functional groups such as ester groups, amino groups, and amide groups. They also stated that nitrogen adsorption/desorption isotherms and pore size distribution curves revealed the new pores of the resulting copolymers were mainly micropores. Fan et al.[42] prepared MARs modified by vinyl groups (a_s, 521 m^2/g; d_p, 100 μm; r_p, 4.1 nm; v_p, 0.79 cm^3/g). Pi[43] prepared methyl acrylate-*co*-divinylbenzene macroporous adsorbents (a_s, 101 m^2/g; d_p, 210 μm; r_p, 2.1 nm) by using a suspension polymerization process. Apparently, the surface areas of these modified MAR adsorbents were not very high, and their pore sizes mainly came from the microporous structure. It is well-known that the microporous structure of an adsorbent is unfavorable in adsorption applications even though the MARs with vinyl groups has a much higher surface area. Besides, it is suspicious that the modified MARs have good thermal stability and could be resistant to a basic corrosion because of the existence of acrylate-*co*-divinylbenzene on the surface. Our previous study[31] showed that the thermal stability of acrylate-*co*-divinylbenzene was not good enough and the drying temperature above 373 K would destroy the pore of the resin and make the pore collapse. The destroyed pore can make unfavorable physical structure, and this would doubtless have undesirable adsorption consequences. We think it should, at least, be classified as another adsorbent material rather than a prevalent modified MAR. Being different from conventional MAR composites, Mim/MAR composite is a full RTIL surface adsorbent. Therefore, it has relatively high specific surface area and pore volume, which make it be able to be coated and bonded with a sufficient amount of flavonoid molecules in the adsorption process.

Pore Nature. The pore nature of the adsorbent plays a very important role in the efficiency of the adsorption process. The pore nature of an adsorbent depends on its pore structure and pore size distribution. According to IUPAC recommendations,[44] the pores are classified as micropores (widths below 2 nm), mesopores (between 2 and 50 nm), and macropores (above 50 nm). Pore size distribution of an adsorbent is generally measured by the desorption branch of the isotherm, and pore structure is usually evaluated by the shape of the adsorption/desorption isotherm.

Nawrocki[40] and Jaroniec[45] explained the relationship between isotherm shape and pore structure and pore size distribution. In brief, a porous adsorbent having a type IV isotherm with an H1 hysteresis loop is most favorable for adsorption purposes. The type is associated with capillary condensation taking place in mesopores and is characteristic of a material composed of agglomerates of approximately uniform spheres in a fairly regular array and having a narrow distribution of pore sizes.

The capillary effect in the adsorption of the synthetic MARs was tested. Figure 4 shows the relationship between Q_e and C_e of synthetic MARs. It also could be found that the variation of Q_e and C_e was not positive-going. The adsorption features of MARs are determined by their structure and the special preparation. Furthermore, special pore structure makes MARs present properties that are obviously different from those of other adsorbents. Due to the existence of many capillaries with different pore diameters in MARs and the special adsorption process, the capillary effect should take place inevitably during the adsorption. Thus, the waves of C_e could be attributed to the capillary effect during the intersection of the adsorption stage.

Many previous papers have described the adsorption of MARs by the Langmuir and Freundlich patterns, and the capillary effect was not found in earlier studies. One of the major reasons might be that the capillary effect was covered up. The infiltrated solution would play an important role in the capillary effect. According to the soakage principle, if the solution was infiltrated to MAR, capillary elevation would take place. Thus, the adsorbate would enter into all accessible pores of MARs more smoothly and be adsorbed on the inner surface of these pores. As a result, if there was no accumulation of adsorbate in solution, C_e would increase monotonously with the increase of concentration or volume, and the capillary effect would be covered up. On the contrary, if solution was not infiltrated to MAR, the adsorbate's entry into MARs would be hampered from larger pores to smaller pores; thus, the concentration of bulk solution would increase, which coincided with our previous research.[31]

In conventional methods, some undesirable characteristics appeared. MARs very often show a wide pore size distribution. The phenomenon that adsorption feature of original MARs in Figure 5 did not show obvious capillary effect indicated that the isotherm of original MARs was a type IV isotherm with a hysteresis loop intermediate between H2 and H3.[38,45] This type of hysteresis loop suggests the pores are "ink bottle" shape,[46] which offers inefficient adsorption due to the slow diffusion of solute and solvent molecules into and out of these pores. Da's group work confirmed the phenomenon.[47] Furthermore, for conventional techniques, there is a contradiction between high surface area and appropriate pore structure. As described above, when the MARs are not modified, micropores are predominately formed; if the RTILs are grafted on the MARs, the synthetic materials would have better physical structure, but while the temperature is high, surface area and pore volume decrease sharply. Unfortunately, much loss in surface area and pore volume cannot be compensated by better or profitable pore structure.

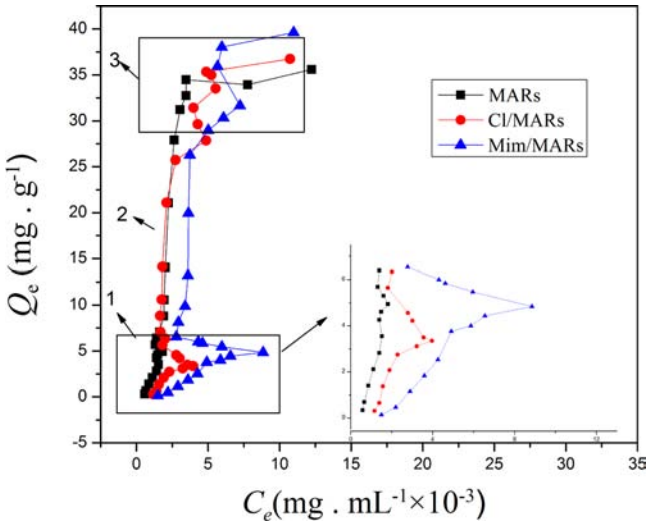

Figure 5. Adsorption capillary effect of MARs, Cl/MARs, and Mim/MARs (n = 3).

Low pore volume, wide pore size distribution, and unfavorable pore structure of MARs make it necessary to develop a new method. Wang and co-workers[48] have attempted to solve the problem by using synthetic MARs at 383 K. However, a significant reduction of total surface area and total pore volume accompanied the improvement of pore structure by this method.

The core−shell structure and RTIL employed procedure can greatly diminish or overcome the above drawbacks. It achieved the goal without loss of surface area and pore volume. As shown in Figure 3a, the isotherm of Mim/MAR particles is a type IV adsorption isotherm. The type of isotherm is characteristic of a mesoporous adsorbent. Furthermore, the hysteresis loop is of type H1. This means the pore structure of Mim/MARs particles is cylindrical, which have good pore connectivity and relatively narrow pore size distributions. The pore size distribution mainly locates in a mesoporous zone (Figure 4b), a relatively narrow range compared with most MARs. As was mentioned earlier, the narrow pore size distribution in the mesopore range is desirable for the applications of organics as adsorbent. The cylindrical mesopores allow rapid and unhindered solution and solute molecules, favorable for high adsorption efficiency. Thus, the pore size of synthetic adsorbents has a type IV isotherm with an H1 hysteresis loop, which is most favorable for adsorption purposes.

Particle Size Distribution. Adsorption properties of adsorbent are influenced not only by their surface area and pore structure but also by the size of their particles, especially by their particle size distribution. The particle size and particle size distribution of MARs depend on a modified process. Different MARs are different in their particle size distribution. Nonpolar MARs reported in ref 15 are prepared from 0.115 to 1.25 mm in diameter. Poorly polar and stronglu polar MARs are prepared from 0.300 to 1.27 mm.

MARs always have low density, although the value is varied from different resources. Commonly, apparent density of MARs is about the same as that of *N*-methylimidazole. This makes it easy to classify the particles into narrow distribution. Moreover, one of the important features of the modified technique is the uniformity of the resulting particles. Particle size and particle size

distribution of core−shell material are determined by the dimensions of the core materials employed. The more uniform the cores are, the narrower the particle size distribution of the Mim/MAR spheres. The average diameter of unclassified Mim/MARs is 1.2 mm with a standard deviation of 0.106 mm. As described under Results the standard deviations for both core spheres are almost the same; this indicates the uniformity of *N*-methylimidazole coatings. Mim/MAR spheres have much narrower particle size distribution than modified MARs prepared by conventional methods, and the narrow distribution would benefit the adsorption efficiency of flavonoids.

Chemical Stability. The chemical stability of MARs is an important parameter in the adsorption process, especially for some specific objects. Interest in application of RTILs as an alternative support for MARs is mainly due to their excellent chemical properties and chemical stability. Prior research has confirmed that RTILs are very stable between pH 1 and 14, and MARs for active components from natural plants were stable up to pH 6. Jiang's group has developed stable RTIL-based stationary phases or additions in mobile phase for HPLC.[26,27]

The chemical stability of Mim/MARs under acidic condition was tested by immersing 2 g of Mim/MARs into a solution of 100 mL of hydrochloric acid and holding it for 3 days. Elemental construction of the synthetic material was detected by Vario EL to confirm that the Mim/MARs were efficiently stabilized. This indicates that the MAR core materials were efficiently protected. Mim/MAR adsorbent was prepared in a solution containing *N*-methylimidazole. During the modified process, while Mim piled up and grafted onto the matrix of the MARs to form shell porous materials, *N*-methylimidazole ions adsorbed and grafted inside the MAR pore and on the surface to form a Mim shielding film.

Flavonoid Adsorption Application. In flavonoid adsorption, a resin with high surface area, high pore volume, and good chemical stability is desirable. For any adsorption, there should be an optimum loading amount of adsorbent. In our experiment, this amount is a measure of uniformly and minimally MAR grafted RTILs and depends on the resins' specific surface area and pore volume.

A comparison between different kinds of MARs is given in Figure 6. The adsorption capacity onto HPD722 (31.33 mg/g) is larger than that of original MARs (23.50 mg/g) due to its appropriate pore size (120 Å) for the flavonoids. The pore size of the original MARs was 51 Å, which is less than the appropriate pore size for flavonoids. Research in the area of physical adsorption on solid materials showed that the adsorption capacity is usually related to the pore size of the adsorbent. The smaller pore size would restrain the entrance of the flavonids into the pores. However, the much larger pore size would weaken the adsorption-driven force of the adsorbate in the adsorption process due to the large space. Moreover, the screen fractionation of the MARs would also be eliminated, and more impurities could also enter into the pores to occupy the adsorption site; thus, the adsorption capacity and sample purity of the flavonoids could reduce obviously. Usually, the ideal pore size is 3−6 times larger than the size of the adsorbent, and thus the adsorption and separation capacity of flavonoids onto the HPD722 are better than the ones onto original MARs. However, the adsorption capacity of adsorbent from aqueous solution is dominated by many factors.[49,50] In this solution system, the adsrbate−adsrbent interaction, specific surface area, and hydrophobicity would also play an important role. Thus, conventional MARs could not supply sufficient adsorbent, limiting the adsorption efficiency and showing low surface area, low pore volume, and poor pore structure, leading to the decrease in selectivity and separation for flavonoids. It is clear that the conventional adsorbent, HPD722, without a hydrogen group, expressed poor selectivity to flavone compounds for their low pertinence to the structural characteristics of flavonids. Introducing hydrogen groups, which were able to form a hydrogen bond between phenolic hydroxyl and flavonoids, could increase their selectivity.

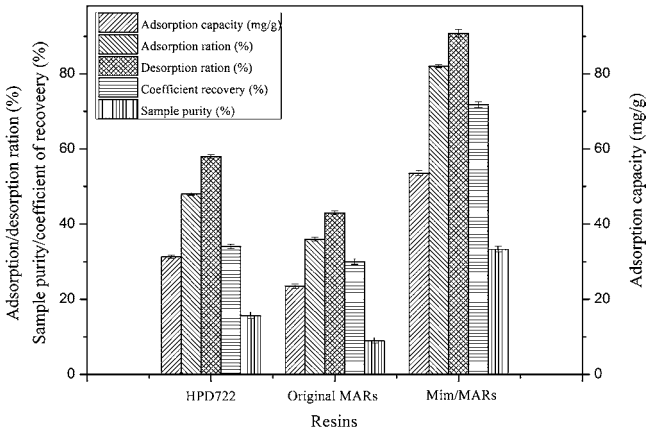

Figure 6. Purification results of HPD722, MARs, and Mim/MARs toward total flavonoids at 303 K (n = 3).

The synthetic MAR, Mim/MAR, has the functional hydrogen-bonding groups *N*-methylimidazole, and its pore size was 122 Å. Thus, the adsorption capacity and purification effect of Mim/MARs were higher than those of HPD722 shown in Figure 6. Thus, the adsorption capacity onto Mim/MARs is 53.52 mg/g, which is much more suitable to adsorption application than the other MARs. For sample solution in our research, a favorable adsorption/desorption ratio to flavonoids was 82 or 91%, about 2 times larger than that of original MARs. In our opinion, the poor adsorption ability of common MARs first results from their improper pore size according to adsorption theory. The second significant contributor to coefficient recovery may be the poor pore structure of MARs. Wide pore size distribution and sometimes poorly shaped pores of MARs are, to some certain degree, disadvantageous to good adsorption capacity due to slow mass transfer. Moreover, the adsorption driving force is another important factor in the adsorption process. Good adsorption is always associated with high pore volume, porosity, and rational driving force. The data in Table 1 appear to support this postulation.

The adsorption capacity of flavonoids on Mim/MARs is better than that on original MARs and HPD722 because of the uniformity of particles, high pore volume, narrow pore size distribution, good pore structure, and composite action of certain molecular interactions. The properties of the synthetic MARs could be controlled by changing the synthetic conditions, and the adsorption results of some other active component from natural plants will be systemically investigated in future research.

Adsorption Kinetics. To illustrate better the adsorption properties of the synthetic copolymer, equilibrium adsorption kinetics of rutin on synthetic resin original MARs and Mim/MARs was investigated at 308 K.

In this paper, we compare three different models to fit the experimental data. The first two are Lagergren pseudo-first-order and pseudo-second-order models that assume reaction rates are proportional to the concentration of solution. Fan and Wang

Table 2. Kinetic Parameters of Pseudo-First- and Pseudo-Second-Order Models onto Original MARs and Mim/MARs

		pseudo-first-order model				pseudo-second-order model			
adsorbent	q_e (exptl) (mg/g)	K_1 (min^{-1})	q_e (calcd)(mg/g)	R^2	Err	K_2 (g/mg min)	q_e (calcd)(mg/g)	R^2	Err
original MARs	11.72	0.0092 ± 0.00072	8.50 ± 1.396	0.8740	0.734	0.00035 ± 0.000028	15.15 ± 0.993	0.9884	0.307
Mim/MARs	32.90	0.0898 ± 0.00644	96.12 ± 10.117	0.5351	15.70	0.03582 ± 0.005279	3.44 ± 0.791	0.7552	5.088

apply this model to fit the adsorption kinetics of phenol on polymeric adsorbent.[39] Table 2 shows the pseudo-first and pseudo-second fits for the adsorption kinetics of flavonoids on original MARs and Mim/MARs from a 2.24 g/L sample solution. Note that there are significant deviations from these models, especially on Mim/MARs. We defined Err as the deviation of fitted coverage from experimental data as

$$\mathrm{Err} = \left[\frac{1}{n_t}\sum_{i=1}^{n_t}(\theta_f(t_i) - \theta_e(t_i))^2\right]^{1/2} \quad (7)$$

where $\theta_f(t_i)$ is the fitted coverage at time t_i, $\theta_e(t_i)$ is the experimental coverage ($\theta_e(t_i) = \Delta f(t_i)/\Delta f_{max}$, where $\Delta f(t_i)$ is the frequency shift at time t_i and Δf_{max} is the final maximum frequency shift), and n_t is the total number of data points.[45]

Table 2 summarizes the resulting pseudo-first and pseudo-second model fits. It shows that all of the deviations from the pseudo-first models are bigger. On the other hand, when resins are modified with *N*-decylimidazole, there is the biggest deviation from these models (Err has the larger value). Considering that Mim/MARs have the larger specific areas and better pore structure, the equilibrium rate of flavonoids on Mim/MARs is much higher than that of original MARs, and Table 2 suggests that the desorption section has to be taken into account; the Lagergren kinetics model does not fit well in this case because these two classical models were produced to describe kinetics of reactions, not adsorption or desorption.

The third model is a first-order, two-component model that assumes the adsorption process contained two compartments. Valderrama and Lao used the two-component model to fit the adsorption kinetics of polyaromatic hydrocarbons on activated carbon and polymer resins.[51] Table 3 shows the parameters of fit

Table 3. Kinetic Parameters of Two-Component Models onto Original MARs and Mim/MARs

resin	origianl MARs	Mim/MARs
χ^2/DoF	2.285	1.847
F_1	6.9498	22.4827
K_1	0.0188	0.00150
F_2	6.3804	12.9270
K_2	0.000960	0.0000145
R^2	0.9665	0.9869
Err	0.5545	0.6411

on original MARs and Mim/MARs from a 2.24 g/L sample solution. It seemed that this model containing two compartments of adsorption is more reasonable. However, it could be found that R^2 and χ^2/DoF of the two-compartment model are not ideal. Moreover, more explicit explanations of an adsorption process are the ultimate aim of kinetics study, and this model still lacks some detailed parameters of sphere size to explain the process.

New Adsorption Kinetics Model: Sphere-Size Model. According to the results of the above three adsorption kinetics models, we have developed a new adsorption kinetics model that takes sphere size and multiple components into consideration explicitly. We model the process of adsorption of flavonoids from solution to adsorption resins as follows:

(a) The adsorption process contains more than two steps with differences between quick adsorption, slow adsorption, and slower adsorption.

(b) The adsorption process contains some extensional delivery parameters, which have obvious physical significance and could explain the adsorption more distinctly. These parameters could be calculated quantitatively, respectively, not using a constant.

(c) The rate of an adsorption process is decided by many factors, and the important one is sphere size. The terminated compartments of the adsorption process are determined by polarity inductive effect model. The effect of pore size on different layers of adsorption is analyzed by the terminated compartments and the new sphere-size model.

The complex transport behavior of liquids in polymers has been studied extensively for over 60 years and reviewed by several authors.[52−54] It is now widely agreed that transport involves both a diffusion process, controlled by a concentration gradient, and a relaxation process, controlled by a time-dependent response of the polymer to a stress. As the relative contributions of these two processes change and interact, a wide range of behaviors can be encountered. The observed effects may vary not only with the particular polymer system considered but also with the range of adsorbent size covered in specific experiments.

Comparison of experimental data with Fick's law requires a solution of the diffusion equation appropriate to the sample geometry and experimental boundary conditions. The simplest geometry for powders is the collection of spherical particles of uniform size. This condition can, in fact, be closely approached in specific powders prepared by emulsion polymerization. Consequently, as a model to approximate adsorption of flavonoids by synthetic resins, we made a new model for the adsorption on nonuniform resins in the case of uniform initial concentration through the sphere, a constant concentration at the surface, and constant D_r.

According to the theory of the first-order, two-component, four-parameter model, the equation of a new model consisting of sphere size is

$$\frac{M_t}{M_0} = F_1\, e^{-4\times 2^2\pi^2 D_{r1} t/r_1^2} + F_2\, e^{-4\times 2^2\pi^2 D_{r2} t/(r_1+r_2)^2} \quad (8)$$

where M_t is the solid-phase sorbate concentration at a given time, M_0 is the initial solid-phase sorbate concentration, F_1 and F_2 are different compartment fractions, D_{r1} (10^{-13} cm^2/s) and D_{r2} (10^{-15} cm^2/s) are the adsorbate diffusion coefficients in the polymer in different adsorption compartments, and r_1 and r_2 are the diameter of the sphere (mm) on which the different compartments of the adsorption process are mainly carried out.

However, it should be noted that this first-order, two-component, four-parameter model does not necessarily consider

dx.doi.org/10.1021/jf300633g | J. Agric. Food Chem. 2012, 60, 6546−6558

Table 4. Regression Result Based on the Induction Force Transfer Effect

resin	layer	χ^2/DoF	Q_m(mg/g)	K_1(L/mg)	K_2(L/mg)	K_3(L/mg)	K_4(L/mg)	K_5(L/mg)	R^2
original MARs	1	1.2531	32.530	0.0399	0.0372				0.979
	2	1.0134	54.073	0.0156	0.0712	0.0094			0.987
	3	1.0006	7.2553	0.4135	0.1045	0.2311	0.0014		0.989
	4	0.2031	3.7234	0.3612	0.1982	0.0235	0.0044	5.67×10^{-4}	0.994
Mim/MARs	1	2.3792	60.787	0.0408	0.0204				0.945
	2	0.7779	15.132	0.0364	0.0272	0.0124			0.987
	3	0.2161	11.181	0.6174	0.0274	0.0201	0.0051		0.994
	4	0.3263	4.178	0.0182	1.09×10^{-3}	4.74×10^{-3}	0.0767	0.0286	0.989

Table 5. Kinetic Parameters of the New Sphere-Size Models onto Original MARs and Mim/MARs

	origianl MARs				Mim/MARs			
	layer 1	layer 2	layer 3	layer 4	layer 1	layer 2	layer 3	layer 4
χ^2/DoF	22.8061	0.6872	0.3821	0.3033	11.2702	2.0465	1.8751	1.8574
F_1	4.6231	9. 2485	8.1770	9.4095	8.8907	16.4627	20.8970	18.3986
D_1	3.7500	2.4762	3.0012	1.4641	2.8646	9.3095	5.5156	3.2487
r_1	0.2718	0.2525	0.3095	0.6479	0.7441	0.8774	0.8352	1.2768
F_2		9.0277	7.1865	8.8815		16.6199	11.3224	18.2658
D_2		1.0450	8.2550	3.9548		1.8505	3.7916	1.7472
r_2		0.2315	0.1137	0.3409		1.1780	0.4610	0.8825
F_3			1.4338	1.5161			2.0802	2.6892
D_3			6.3069	4.5671			1.8720	9.6105
r_3			0.0801	0.1181			0.2168	0.2319
F_4				0.5242				2.6609
D_4				5.9438				2.6476
r_4				0.0307				0.039
R^2	0.7528	0.9949	0.9950	0.9964	0.7117	0.9963	0.9970	0.9970
Err	1.8036	0.2578	0.2559	0.1949	5.7168	0.6411	0.5705	0.5679

the reasonable procedures of adsorption. The model defining the adsorption process contained just two steps without taking into account the differences between fast adsorption, slow adsorption, and even slower adsorption.[55−57] In this work, considering the restriction above, a new modified model of adsorption kinetics with sphere size was created according to Karickhoof's theory[58] and multiparameter adsorption kinetics model.[24] The pattern in which the adsorption process should contain more compartments was proposed, the real sections were investigated through polarity inductive effect model, and the effect of pore size on different layers was analyzed by the new model through the experimental results.

The equation of the new model with sphere size for more compartments is

$$\frac{M_t}{M_0} = F_1\, e^{-4\times n^2\pi^2 D_{r1} t/r_1^2} + F_2\, e^{-4\times n^2\pi^2 D_{r2} t/(r_1+r_2)^2} + F_3\, e^{-4\times n^2\pi^2 D_{r3} t/(r_1+r_2+r_3)^2} + \ldots + F_n\, e^{-4\times n^2\pi^2 D_m t/(r_1+r_2+r_3+\ldots+r_n)^2} \quad (9)$$

The equation denotes a general equation of adsorption delivered to the nth level. Thus, the transmission of the delivery and the effect of sphere size could be investigated from the adsorption equilibrium by Origin 8.1.

The terminated layer of the adsorption is determined by the multilayer polarity inductive effect model in Table 4. The equation of the model and the regression results are shown as follows:

$$\frac{Q_e}{Q_m} = \left\{K_1C_e\{(1 - K_iC_e)\sum_{i=3}^{i}[K_1C_e + 2K_1K_2C_e^2 + \ldots + (i-3)K_1K_2\ldots K_{i-2}C_e^{i-1}] + (i-2)K_1K_2\ldots K_{i-1}C_e^{i-1}(1 + K_iC_e - K_{i+1}C_e)\} + K_1K_2\ldots K_iC_e^{i-1}\right\} \Big/ \left\{(1 - K_{i+1}C_e)[(1 + K_{i-1}C_e)\sum_{i=3}^{i}(1 + K_iC_e - K_{i+1}C_e^2) + K_1K_2\ldots K_{i-2}C_e^{i-2}(1 + K_{i-1}C_e - K_iC_e)]\right\} \quad (10)$$

It could be found that R^2, Q_m, and χ^2/DoF were best after regression to the fourth layer for original MARs and to the third layer for Mim/MARs. Furthermore, the values of χ^2/DoF were all much lower than the beginning ones. All of this showed that the induction force of the adsorbent would transmit to the fourth layer on original MARs and to the third layer for Mim/MARs. The different kinds of MARs would have different induction force layers. In this work, the functionalized part of the modified resins plays a key role in the adsorption process, and its driving force is obviously higher than the ones in later layers; the one in

dx.doi.org/10.1021/jf300633g | J. Agric. Food Chem. 2012, 60, 6546−6558

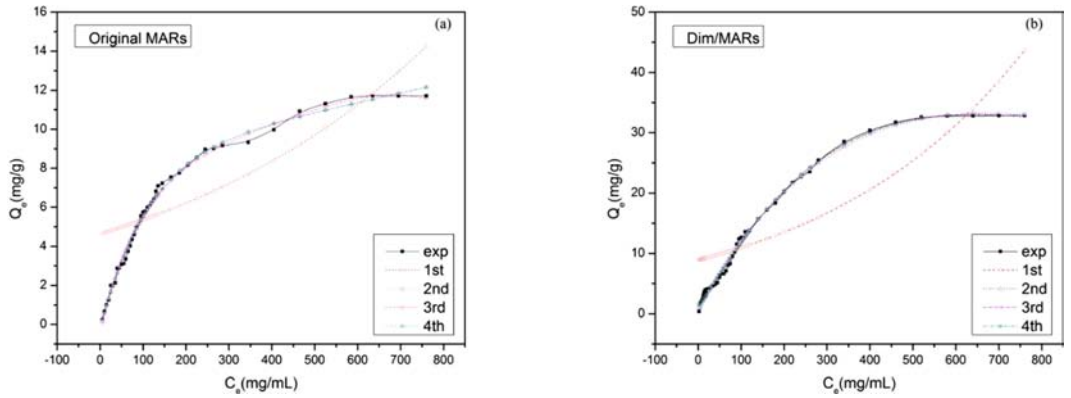

Figure 7. Regression cruves of the relationship between adsorption amount and time: (a) new sphere-size model fit for the adsorption kinetics of flavonoids onto original MARs; (b) new sphere-size model fit onto Mim/MARs.

the fourth layer could be ignored compared with the one in the shell part. However, the phenomenon would not be produced onto original MARs due to the nonfunctioned structure, and the difference between K_1 and K_2 of the fourth layer on original MARs is much lower than the one onto modified MARs. Thus, a conclusion of regressions by multilayer polarity inductive effect model is that the number of transmitted layer onto original MARs is four and the number onto Mim/MARs is three.

The effect of sphere size on an adsorption process is determined by the new adsorption kinetics model and the terminated driving force layers. The results of the regression are shown in Table 5 and Figure 7.

It could be found that R^2 and χ^2/DoF of the new adsorption kinetics model consisting of sphere sizes are the same as the result of our multiparameter adsorption kinetics model. The adsorption process was distinctly divided into four steps onto original MARs and three steps onto Mim/MARs because the r_n value of each system was lower than the corresponding r_{n-1} value. For all test systems, the largest F_1 value of the first adsorption fraction was for Mim/MARs and the smallest F_4 value of the fourth fraction was for original MARs. The adsorption parameters of all three compartments were strong functions of the sphere-size distribution. For original MARs, the four compartments of adsorption are mainly on spheres of sizes >0.65, 0.65−0.34, 0.34−0.12, and 0.03−0.12 mm, respectively, and three compartments onfspheres >0.83, 0.46−0.83, and 0.22−0.46 mm for Mim/MARs. The effect of the special spheres, smaller than 0.03 mm for original MARs and 0.22 mm for Mim/MARs, could be ignored compared with the one in the first layer.

These results indicated that (1) the extent of rapid adsorption is more prominent on Mim/MARs because of its dominant macropores structure, high specific surface area, obvious hydrogen bond, and characteristic property of ionic liquid grated on the core resins. (2) The adsorption processes on original MARs are limited mainly by the fourth adsorption attributed to its abundant microspore structure and are not very hydrophobic. (3) Our new adsorption kinetics model could describe the effect of sphere size on adsorption kinetics well. (4) The result shows that the adsorbed force of the adsorbent transmits to the fourth level onto original MARs and to the third level onto Mim/MARs, which is in accordance with the result of the multilayer polarity inductive effect model. The roles of surface chemistry, hydrophobicity, and some other adsorbent parameters, such as pore size and polarity, upon adsorption and the accompanying kinetics will be systemically investigated in future research.

Regeneration Test. Reproducibility is another important factor that has been neglected so far in the preparation of MARs for adsorption. In experiments, continuous adsorption−regeneration runs of an identical synthetic Mim/MARs were also performed to test its applicability. The superposition of flavonoid adsorption curves in the first and fifth cycles shown in Figure 8 indicates that synthetic resins can be completely regenerated for repeated use without any significant capacity loss, which is significant for practical application.

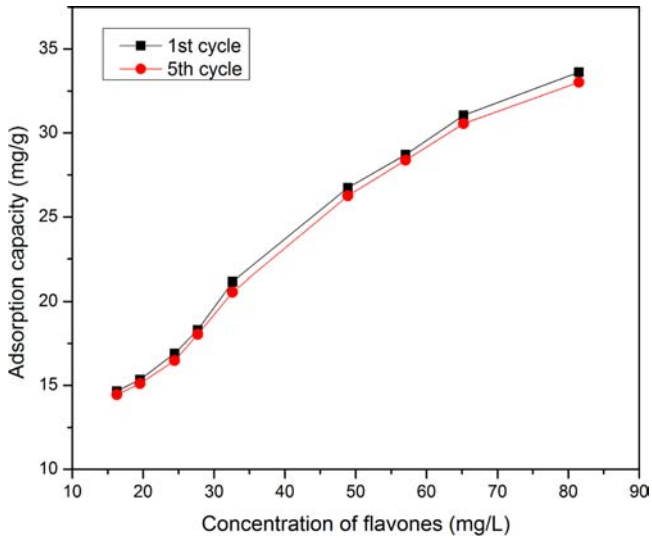

Figure 8. Breakthrough curves of flavone adsorption onto Mim/MARs at 30 °C (first and fifth cycles).

AUTHOR INFORMATION

Corresponding Author

*Phone: +86-931-496-8248. Fax: +86-931-827-7088. E-mail: didl@licp.cas.cn.

Funding

This research project was financially supported by the Hundred Talents Program of the Chinese Academy of Sciences (CAS) and the National Natural Sciences Foundation of China (NSFC, no. 20974116).

Notes

The authors declare no competing financial interest(s).

REFERENCES

(1) Yang, B.; Kalimo, K. O.; Tahvonen, R. L.; Mattila, L. M.; Katajisto, J. K.; Kallio, H. P. Effect of dietary supplementation with sea buckthorn (*Hippophae rhamnoides*) seed and pulp oils on the fatty acid composition of skin glycerophospholipids of patients with atopic dermatitis. *J. Nutr. Biochem.* **2000**, *11* (6), 338−340.

(2) Zu, Y. G.; Li, C. Y.; Fu, Y. J.; Zhao, C. J. Simultaneous determination of catechin, rutin, quercetin kaempferol and isorhamnetin in the extract of sea buckthorn (*Hippophae rhamnoides* L.) leaves by RP-HPLC with DAD. *J. Pharm. Biomed. Anal.* **2006**, *41* (3), 714−719.

(3) Arimboor, R.; Venugopalan, V. V.; Sarinkumar, K.; Arumughan, C.; Sawhney, R. C. Integrated processing of fresh Indian sea buckthorn (*Hippophae rhamnoides*) berries and chemical evaluation of products. *J. Sci. Food Agric.* **2006**, *86* (14), 2345−2353.

(4) Zadernowski, R.; Naczk, M.; Nesterowicz, J. Phenolic acid profiles in some small berries. *J. Agric. Food Chem.* **2005**, *53* (6), 2118−2124.

(5) Dong, T. T. X.; Zhao, K. J.; Gao, Q. T.; Ji, Z. N.; Zhu, T. T.; Li, J.; Duan, R.; Cheung, A. W. H.; Tsim, K. W. K. Chemical and biological assessment of a Chinese herbal decoction containing radix astragali and radix angelicae sinensis: determination of drug ratio in having optimized properties. *J. Agric. Food Chem.* **2006**, *54* (7), 2767−2774.

(6) Gao, Q. T.; Cheung, J. K. H.; Li, J.; Chu, G. K. Y.; Duan, R.; Cheung, A. W. H.; Zhao, K. J.; Dong, T. T. X.; Tsim, K. W. K. A Chinese herbal decoction, danggui buxue tang, prepared from radix astragali and radix angelicae sinensis stimulates the immune responses. *Planta Med.* **2006**, *72*, 1227−1231.

(7) Gao, X. Q.; Ohlander, M.; Jeppsson, N.; Bjork, L.; Trajkovski, V. Changes in antioxidant effects and their relationship to phytonutrients in fruits of sea buckthorn (*Hippophae rhamnoides* L.) during maturation. *J. Agric. Food Chem.* **2000**, *48*, 1485−1490.

(8) Cheng, J. Y.; Kondo, K.; Suzuki, Y.; Ikeda, Y.; Meng, X. S.; Umemura, K. Inhibitory effects of total flavonoids of *Hippophae rhamnoides* L. on thrombosis in mouse femoral artery and in vitro platelet aggregation. *Life Sci.* **2003**, *72*, 2263−2271.

(9) Geetha, S.; Ram, M. S.; Singh, V.; Ilavazhagan, G.; Sawhney, R. C. Anti-oxidant and immunomodulatory properties of sea buckthorn (*Hippophae rhamnoides*)-an in vitro study. *J. Ethnopharmacol.* **2002**, *79*, 373−378.

(10) Du, X. L.; Yuan, Q. P.; Li, Y.; Zhou, H. H. Preparative purification of solanesol from tobacco leaf extracts by macroporous resins. *Chem. Eng. Technol.* **2008**, *31* (1), 87−94.

(11) Li, J.; Chase, H. A. Use of expanded bed adsorption to purify flavonoids from *Ginkgo biloba* L. *J. Chromatogr., A* **2009**, *1216* (50), 8759−8770.

(12) Ye, J. H.; Jin, J.; Liang, H. L.; Lu, J. L.; Du, Y. Y.; Zheng, X. Q.; Liang, Y. R. Using tea stalk lignocellulose as an adsorbent for separating decaffeinated tea catechins. *Bioresour. Technol.* **2009**, *100* (2), 622−628.

(13) Fu, B. Q.; Liu, J.; Li, H.; Li, L.; Lee, F. S. C.; Wang, X. R. The application of macroporous resins in the separation of licorice flavonoids and glycyrrhizic acid. *J. Chromatogr., A* **2005**, *1089* (1−2), 18−24.

(14) Kammerer, J.; Boschet, J.; Kammerer, D. R.; Carle, R. Enrichment and fractionation of major apple flavonoids, phenolic acids and dihydrochalcones using anion exchange resins. *LWT−Food Sci. Technol.* **2011**, *44* (4), 1079−1087.

(15) Baycin, D.; Altiok, E.; Ulku, S.; Bayraktar, O. Adsorption of olive leaf (*Olea europaea* L.) antioxidants on silk fibroin. *J. Agric. Food Chem.* **2007**, *55* (4), 1227−1236.

(16) Antonio, P.; Iha, K.; Suarez-Iha, K. Adsorption of di-2-pyridyl ketone salicyloylhydrazone on silica gel: characteristics and isotherms. *Talanta* **2004**, *64* (2), 484−490.

(17) Liu, Y. F.; Liu, J. X.; Chen, X. F.; Liu, Y. W.; Di, D. L. Preparative separation and purification of lycopene from tomato skins extracts by macroporous adsorption resins. *Food Chem.* **2010**, *123* (4), 1027−1034.

(18) Crittenden, J. C.; Sanongraj, S.; Bulloch, J. L.; Hand, D. W.; Rogers, T. N.; Speth, T. F.; Ulmer, M. Correlation of aqueous-phase adsorption isotherms. *Environ. Sci. Technol.* **1999**, *33* (17), 2926−2933.

(19) Huang, W.; Xue, A.; Niu, H.; Jia, Z.; Wang, J. Optimised ultrasonic-assisted extraction of flavonoids from folium eucommiae and evaluation of antioxidant activity in multi-test systems in vitro. *Food Chem.* **2009**, *114* (3), 1147−1154.

(20) Zhu, X. X.; Banana, K.; Yen, R. Pore size control in cross-linked polymer resins by reverse micellar Imprinting. *Macromolecules* **1997**, *30* (10), 3031−3035.

(21) Hennion, M. C. Graphitized carbons for solid-phase extraction. *J. Chromatogr., A* **2000**, *885*, 73−95.

(22) Shetty, P. H.; Youngberg, P. J.; Kersten, B. R.; Poole, C. F. Solvent properties of liquid organic salts used as mobile in microcolumin reversed-phaseliquid-chromatography. *J. Chromatogr.* **1987**, *411*, 61−79.

(23) Roesch, D.; Bergmann, M.; Knorr, D.; Kroh, L. W. Structure-antioxidant efficiency relationships of phenolic compounds and their contribution to the antioxidant activity of sea buckthorn juice. *J. Agric. Food Chem.* **2003**, *51* (15), 4233−4239.

(24) Carmichael, A. J.; Earle, M. J.; Holbrey, J. D.; McCormac, P. B.; Seddon, K. R. The Heck reaction in ionic liquids: a multiphasic catalyst system. *Org. Lett.* **1999**, *1* (7), 997−1000.

(25) Yanes, E. G.; Gratz, S. R.; Baldwin, M. J.; Robison, S. E.; Stalcup, A. M. Capillary electrophoretic application of 1-alkyl-3-methylimidazolium-based ionic liquids. *Anal. Chem.* **2001**, *73* (16), 3838−3844.

(26) Zhang, W. Z.; He, L. J.; Gu, Y. L.; Liu, X.; Jiang, S. X. Effect of ionic liquids as mobile phase additives on retention of catecholamines in reversed-phase high-performance liquid chromatography. *Anal. Lett.* **2003**, *36* (4), 827−838.

(27) Qiu, H. D.; Jiang, S. X.; Liu, X. *N*-Methylimidazolium anion-exchange stationary phase for high-performance liquid chromatography. *J. Chromatogr., A* **2006**, *1103* (2), 265−270.

(28) Berens, A. R.; Huvard, G. S. Particle size distribution of polymer powders by analysis of sorption kinetics. *J. Dispersion Sci. Technol.* **1981**, *1*, 359−378.

(29) Berens, A. R. Diffusion and relaxation in glassy polymer powders: 1. Fickian diffusion of vinyl chloride in poly(vinyl choride). *Polymer* **1977**, *18*, 697−704.

(30) Carroll, K. M.; Harkness, M. R.; Bracco, A. A.; Balcarcel, R. R. Application of a permeant/polymer diffusional model to the desorption of polychlorinated biphenyls from Hudson River sediments. *Environ. Sci. Technol.* **1994**, *28*, 253−258.

(31) Chen, Z. B.; Zhang, A. J.; Li, J. E.; Dong, F.; Di, D. L.; Wu, Y. Z. Study on the adsorption feature of rutin aqueous solution on macroporous adsorption resins. *J. Phys. Chem. B* **2010**, *114* (14), 4841−4853.

(32) Lou, S.; Chen, Z.; Liu, Y.; Ye, H.; Di, D. New way to analyze the adsorption behavior of flavonoids on macroporous adsorption resins functionalized with chloromethyl and amino groups. *Langmuir* **2011**, *27* (15), 9314−9326.

(33) Liu, Y.; Di, D.; Bai, Q.; Li, J.; Chen, Z.; Lou, S.; Ye, H. Preparative separation and purification of rebaudioside a from steviol glycosides uing mixed-mode macroporous adsorption resins. *J. Agric. Food. Chem.* **2011**, *59* (17), 9629−9636.

(34) Juang, R. S.; Shiau, J. Y. Adsorption isotherms of phenols from water onto macroreticular resins. *J. Hazard. Mater.* **1999**, *70* (3), 171−183.

(35) Kozlov, E. I. Synthsis of vitamin K2/15, K2/20 and their 1-acyloxy-ethers. *Med. Promst. SSSR* **1965**, *14*, 16−21.

(36) Shurmel, L. B.; Shatalov, V. V.; Molchanova, T. V.; Peganov, V. A.; Smirnov, D. I. IR-spectroscopy investigation of the properties of ignites in uranium sorption duribng processing of silicon-containing solutions and pulps. *At. Energy* **2001**, *90*, 218−223.

(37) Chen, Z. B.; Kang, L.; Di, D. L.; Dong, F.; Yu, H. Chloromethylatioin research of LX-1180 macroporous adsorption resin in ultrasonic environment. *Adv. Mater. Res.* **2011**, *233*, 2893−2897.

(38) Sing, K. S. W.; Everett, D. H.; Haul, R. A. W.; Moscou, L.; Pierotti, R. A.; Rouquerol, J.; Siemieniewska, T. Reporting physisorption data for gas solid systems with secial reference to the determination of surface-area and porosity. *Pure Appl. Chem.* **1985**, *57* (4), 603−619.

(39) Wang, H. Y.; Zhao, M. M.; Yang, B.; Jiang, Y. M.; Rao, G. H. Identification of polyphenols in tobacco leaf and their antioxidant and antimicrobial activities. *Food Chem.* **2008**, *107* (4), 1399−1406.

(40) Nawrocki, J.; Rigney, M. P.; McCormick, A.; Carr, P. W. Chemistry of zirconia and its use in chromatography. *J. Chromatogr., A* **1993**, *657* (2), 229−282.
(41) Ren, P.; Zhao, X. L.; Zhang, J.; Shi, R. F.; Yuan, Z.; Wang, C. H. Synthesis of high selectivity polymeric adsorbent and its application on the separation of ginkgo flavonol glycosides and terpene lactones. *React. Funct. Polym.* **2008**, *68* (4), 899−909.
(42) Zeng, X. W.; Fan, Y. G.; Wu, G. L.; Wang, C. H.; Shi, R. F. Enhanced adsorption of phenol from water by a novel polar post-crosslinked polymeric adsorbent. *J. Hazard. Mater.* **2009**, *169* (1−3), 1022−1028.
(43) Zhou, J. C.; Feng, D. W.; Zheng, G. S. Extraction of sesamin from sesame oil using macroporous resin. *J. Food Eng.* **2010**, *100* (2), 289−293.
(44) Caruso, F.; Rodda, E.; Furlong, D. F.; Niikura, K.; Okahata, Y. Quartz crystal microbalance study of DNA immobilization and hybridization for nucleic acid sensor development. *Anal. Chem.* **1997**, *69* (11), 2043−2049.
(45) Jaroniec, C. P.; Jaroniec, M.; Kruk, M. Comparative studies of structural and surface properties of porous inorganic oxides used in liquid chromatography. *J. Chromatogr., A* **1998**, *797* (1−2), 93−102.
(46) Dun, H. J.; Zhang, W. Q.; Wei, Y.; Song, X. Q.; Li, Y. M.; Chen, L. R. Layer-by-layer self-assembly of multilayer zirconia nanoparticles on silica spheres for HPLC packings. *Anal. Chem.* **2004**, *76* (17), 5016−5023.
(47) Li, J.; Chase, H. A. Characterization and evaluation of a macroporous adsorbent for possible use in the expanded bed adsorption of flavonoids from *Ginkgo biloba* L. *J. Chromatogr., A* **2009**, *1216* (50), 8730−8740.
(48) Geng, X. T.; Ren, P.; Pi, G. P.; Shi, R. F.; Yuan, Z.; Wang, C. H. High selective purification of flavonoids from natural plants based on polymeric adsorbent with hydrogen-bonding interaction. *J. Chromatogr., A* **2009**, *1216* (47), 8331−8338.
(49) Tomul, F. Synthesis, characterization, and adsorption properties of Fe/Cr-pillared bentonites. *Ind. Eng. Chem. Res.* **2011**, *50*, 7228−7240.
(50) Xin, L.; Zhang, L. Equilibrium and Do-Do model fitting of water adsorption on four commercial activated carbons with different surface chemistry and pore structure. *Anal. Chem.* **2010**, *82*, 5729−5732.
(51) Valderrama, C.; Cortina, J. L.; Farran, A.; Gamisans, X.; Lao, C. Kinetics of sorption of polyaromatic hydrocarbons onto granular activated carbon and Macronet hyper-cross-linked polymers (MN200). *J. Colloid Interface Sci.* **2007**, *310* (1), 35−46.
(52) Hawthorne, S. B.; Poppendieck, D. G.; Grabanski, C. B.; Loehr, R. C. PAH release during water desorption, supercritical carbon dioxide extraction, and field bioremediation. *Environ. Sci. Technol.* **2001**, *35* (22), 4577−4583.
(53) Chu, B. S.; Baharin, B. S.; Man, Y. B. C.; Quek, S. Y. Separation of vitamin E from palm fatty acid distillate using silica. III. Batch desorption study. *J. Food Eng.* **2004**, *64* (1), 1−7.
(54) El-Dissouky, A.; Elassar, A. Z.; Bu-Olian, A. H. Complex formation, metal uptake, and sorption kinetics of a chemically modified chlorosulfonated polystyrene with aminosalicylic acid. *J. Chem. Eng. Data* **2011**, *56* (5), 1827−1839.
(55) Aleksieva, K.; Xu, J.; Wang, L. M.; Sassi, A.; Pientka, Z.; Zhang, Z. P.; Jerabek, K. Effects of post-crosslinking of macroreticular styrene−divinylbenzene copolymers on their morphology. *Polymer* **2006**, *47* (19), 6544−6550.
(56) Oberholzer, M. R.; Lenhoff, A. M. Protein adsorption isotherms through colloidal energetics. *Langmuir* **1999**, *15* (11), 3905−3914.
(57) Lou, S.; Chen, Z. B.; Liu, Y. F.; Ye, H. L.; Di, D. L. Synthesis of functional adsorption resin and its adsorption properties in purification of flavonoids from *Hippophae rhamnoides* L. leaves. *Ind. Eng. Chem. Res.* **2012**, DOI: /10.1021/ie201494k.
(58) Karickhoff, S. W.; Morris, K. R. Sorption dynamics of hydrophobic pollutants in sediment suspensions. *Environ. Toxicol. Chem.* **1985**, *4* (4), 469−479.